PM3 Geometry Optimization and CNDO/S-CI Computation of UV/Vis Spectra of Large Organic Structures: Program Description and Application to Poly(triacetylene) Hexamer and Taxotere

HAROLD BAUMANN, RAINER E. MARTIN, FRANÇOIS DIEDERICH

Laboratorium für Organische Chemie der Eidgenössischen Technischen Hochschule, Universitätsstrasse 16, CH-8092 Zürich, Switzerland

Received 17 December 1997; revised 29 September 1998; accepted 1 October 1998

ABSTRACT: SIXW.C, a new C version of the computer program CNDUV99 (based on CNDO/S-CI with inclusion of doubly excited configurations) is described and shown to be useful for the computation of the UV/Vis spectra of fairly large molecules. The geometries of the molecules were obtained by our C version of program PM3. To demonstrate the broad applicability of program SIXW.C we have chosen two representative examples: first, a linearly conjugated oligomer of defined length; and, second, a natural product that currently plays a very significant role in cancer therapy. The first molecule is a recently synthesized linearly conjugated monodisperse hexamer of $\sim$4.6 nm in length ($C_{126}H_{222}O_{12}Si_{14}$), with poly(triacetylene) backbone. Despite the 36 conjugated C-atoms of the framework, it exhibits remarkable thermal and environmental stability, which allows in-depth investigation of its physical properties. Therefore, this made it a very attractive candidate for comparison of the theoretically calculated and experimentally measured UV/Vis spectra, as there is still considerable interest in predicting linear optical properties of large conjugated organic molecules at the border to polymers. The agreement between experimental and calculated spectra is better with the UHF-PM3- rather than with the RHF-PM3-optimized structure of the molecule, showing, for the former, excellent agreement between the experimental and theoretical longest wavelength maximum (λ_{max}), which differ by only 16 nm (802 cm^{-1}). This

Correspondence to: H. Baumann; e-mail: baumann@org.chem.ethz.ch

CCC 0192-8651 / 99 / 040396-16

result is of fundamental interest, because the electronic structure reveals a spin-polarized character, usually referred to as spin density wave. In addition to the flat poly(triacetylene) oligomer, we have calculated *N-tert*-butoxycarbonyl-10-deacetyl-*N*-debenzoyltaxol ($C_{43}H_{53}NO_{14}$, taxotere) as an example for a three-dimensional molecule for which, until now, only MM2 force-field computations were performed. It is closely related to the potent inhibitor of cell division, taxol, which was isolated first in 1971 from the stem bark of the yew *Taxus brevifolia Nutt*. Taxotere is one of the key weapons in modern cancer therapy. © 1999 John Wiley & Sons, Inc. J Comput Chem 20: 396–411, 1999

Keywords: poly(triacetylene); taxotere; UV/Vis spectrum; UHF-PM3; CNDO/S-CI; spin density wave

CNDO/S-CI with Inclusion of Doubly Excited Configurations

The presented computer program, SIXW.C (ANSI-C), was developed on the basis of the FORTRAN program, CNDUV99 (CNDO/S-CI with inclusion of doubly excited configurations).[1] The new program enables the computation and graphical representation of the electronic transitions of molecules of, in principle, arbitrary size. By using dynamic memory management it is only limited by speed and memory size of the computer.

The input data are a formatless textfile and, besides some parameters, the Z-matrix is requested, which represents the connectivity of the molecule considered and contains the bond lengths, bond angles, and torsional angles. The actual C version allows the consideration of an arbitrary number of basis orbitals of the s- and p-type, of nuclei, and singly and doubly excited electronic configurations for the CI computation. Only singlet states may be treated. The largest molecule ever computed by our program has the formula $C_{134}H_{178}O_{32}Si_{34}$, and is a 1042-electron system. In this example, 4222 electronic configurations were considered for the CI process. Maintainance of our C program is particularly simple, because it is written in a clearly structured way and does not contain any go-to statements.

The source code was compiled up until now without any changes on the following computer environments: DEC Alpha 21164, Digital Unix Version 4.0B; IBM RS-6000/590, AIX Version 4.1; Cray J90-SE/20/8192, UNICOS 19.0.0.2; Silicon Graphics ONYX 2, Irix Release 6.4 IP 27; Hewlett-Packard Convex Exemplar SPP 2000/X-32, SPP-UX 5.2.1. On the Hewlett-Packard Convex Exemplar SPP 2000/X-32, where the aforementioned very large molecule was computed, the executable of the program SIXW.C has a length of 265 kilobytes (kB). The FORTRAN version of QCPE Program 333,[1b] which is limited to the computation of 50 atoms, 99 orbitals, and 99 configurations, has a length of 599 kB. Most of the actual computations have been performed on the DEC Alpha 21164 machine of our computer cluster. For the computation of the UV/Vis spectrum of the poly(triacetylene) hexamer, this machine needs 14 hours when using 2400 excited electronic configurations for the configuration interaction process. Further details of the new program are described in the Appendix.

Application of Program

POLY(TRIACETYLENE) OLIGOMER 1

Conjugated organic molecules and polymers show great promise as components for advanced electronic and photonic applications,[2] because they possess inherent synthetic flexibility, which allows the design of materials exhibiting specific properties and functions. In addition, conjugated organic molecules of multinanometer length have been widely discussed as being of particular interest for use as molecular wires in the emerging field of molecular electronics.[3] Oligomers of clearly defined length also play an important role in establishing structure–property relationships in the corresponding polymers, as has been widely demonstrated.[4] Therefore, there is an ongoing interest in the theoretical understanding and calculation of large conjugated organic molecules and polymers. In particular, the ''effective conjugation length'' or the ''point of saturation,'' which is the number of repeat units in a conjugated polymer required to furnish size-independent redox, optical, or other properties, is both theoretically and practically a parameter of substantial interest.[5] The oligomer

we have chosen for our calculations is a linearly conjugated oligomer of ~4.6 nm in length with poly(triacetylene) backbone, which has been recently synthesized, and contains 36 conjugated C-atoms.[6]

Poly(triacetylene)s [PTAs, —(C≡C—CR=CR—C≡C)$_n$—] are a new class of linearly conjugated polymers with a nonaromatic all-carbon backbone[7] in the progression, which starts with polyacetylene [PA, —(CR=CR)$_n$—] and poly(diacetylene) [PDA, —(C≡C—CR=CR)$_n$—], and ultimately leads to carbyne [—(C≡C)$_n$—], a linear carbon allotrope that has generated considerable interest within the last 25 years.[8]

Due to the bulky lateral silyl groups, the poly(triacetylene) oligomer **1** exhibits significant thermal and environmental stability, combined with high solubility, in a wide range of common solvents. The ready availability and high solubility of hexamer **1** and the corresponding series of monomer to pentamer has permitted extensive investigation of their physical properties, which has been used to estimate the theoretically predicted converging limit of the maximum absorption wavelength (λ_{max}) in poly(triacetylene)s, experimentally disclosing a value of 7–10 monomer units, depending somewhat on the method of evaluation used.[6]

The existence of a converging limit of the maximum absorption wavelength in series of polyenes with increasing chain length has been a subject of much discussion and controversy. The explanation of the phenomenon by Longuet–Higgins and Salem based on bond alternation was once considered to be the most satisfactory.[9] Nowadays, one considers Hartree–Fock (HF) singlet instability, which leads, for a long polyene, to another time-reversal-invariant closed-shell (TICS or restricted) HF solution that brings along some structural distortion (e.g., bond alternation).[10] Fukutome offered another explanation of the phenomenon.[11] He applied the general HF theory to polyenes without bond alternation and showed that the conventional diamagnetic ground state becomes nonsinglet unstable when the length of the molecule exceeds certain critical values. He presented the axial-spin-density-wave solution (ASDW) and the charge-transfer-wave solution (CTW), which were shown to have undulating spin density or charge density distribution and finite energy gaps between the excited and ground states even in cases of infinite length.

These new solutions of the HF equations according to Fukutome potentially have physical meaning or at least have some relation to properties of great interest such as antiferromagnetism[12] and superconductivity.[13] But, although the molecular structures resulting from the UHF geometry optimization are qualitatively correct, only experiments or high level *ab initio* calculations could ultimately determine if the typical undulating spin density distribution has physical meaning or is an artifact of the one determinant approach.

Fukutome estimated the appearance of the ASDW solution for conjugated ring and chain molecules and found thresholds for rings of about 11 and for chains about 5 conjugated carbon–carbon π bonds.[11] Of course, these two thresholds are only rough estimates and vary in certain limits depending on the theoretical approach. One of us (H.B.) showed, in 1978, that the X-ray crystal structure of [18] annulene with nonalternant π bonds can theoretically only be explained by consideration of electron correlation. This is, in principle, equivalent to the application of the unrestricted HF (UHF) method, which leads to an ASDW solution with nonalternant π bonds for this molecule.[14] Dewar et al. computed for [18] annulene a structure with localized π bonds, which turned out to be an artifact due to the use of the RHF method.[15] This artifact has recently been confirmed by Kertesz et al. by MP2/6-31G* and B3LYP/6-311G* computations.[16] On the basis of this confirmation of Fukutome's prediction for conjugated ring compounds it can be expected that **1** will fall, with high probability, within the category of systems that show an ASDW solution reducing the tendency of bond alternation despite its short triple bonds.

TAXOTERE

Taxotere, a complex natural product, is one of the key weapons in modern cancer therapy. In 1971, antitumoral taxol was isolated by Wani and coworkers from the stem bark of the yew *Taxus brevifolia Nutt*, and its structure and configuration were determined by X-ray analysis of two derivatives.[17] The closely related molecule, *N-tert*-butoxycarbonyl-10-deacetyl-*N*-debenzoyltaxol (taxotere) **2**, was synthesized in 1989 by Guéritte-Voegelein et al.[18] and its X-ray structure[19] confirmed the results found by Wani et al.[17] More recently, several other groups also reported the synthesis of taxol.[17] To the best of our knowledge, up until now, for these large compounds (**2**: $C_{43}H_{53}NO_{14}$, molecular weight 807 Da), only MM2 force-field computations have been performed.[20, 21]

By their nature, MM2 computations cannot give a deeper insight into the electronic structure of these molecules of great interest.

COMPUTATION OF THE STRUCTURES OF COMPOUNDS 1 AND 2

In recent years, one of us (H.B.) has developed several computer programs in ANSI-C that are based on the semiempirical methods MINDO/3, MNDO, and PM3.

All programs exploit dynamic memory management and therefore, in principle, work for molecules of any size as long as the computer's RAM is sufficiently large. These programs will be described in detail elsewhere.

We have undertaken an investigation of the molecular structures and UV/Vis spectra of compounds **1** and **2**. By inspection, we can see that hexamer **1** consists of $6n$ (or 36) conjugated π centers, where n stands for the number of monomer units. To minimize our computational effort, the —Si*tert*—$BuMe_2$ in **1** were replaced by —SiH_3 groups. Compound **2** was chosen as representative of a three-dimensional molecule and, to our knowledge, has not been computed previously by semiempirical methods. The PM3 computed heat of formations for **1** and **2** are presented in Table I. For **1**, we find the lowest heat of formation for the UHF C_i ''delocalized'' structure. We are not able to annihilate the spin contamination energy part for such large structures because the spin annihilation algorithm diverges with increasing size of the molecules despite the use of the strongly improved formulation of the Sanibel coefficients by Pauncz.[22] In other words, although the projected energy would lie even lower, our experience showed that spin contaminated structures are rather realistic where geometrical parameters are concerned.

Figure 1 depicts the structure of poly(triacetylene) **1** and the UHF spin densities at the C centers of the backbone. The numbers indicate for this molecule a spin-polarized electronic structure, or a so-called spin-density wave (SDW), which results from a nonsinglet HF instability. A plus sign indicates an α spin, a minus sign denotes a β spin dominance at the indicated π center. This situation indicates, for the UHF-computed molecular structure, less alternation of the bond lengths in comparison with the RHF-computed one, as can be seen in Figure 2. The SDW has been subject of experimental research activities for about 20 years and was observed for the first time in some low-dimensional organic conductors as the low-temperature nonmetallic phase below the transition temperature, T_c.[23] Several reviews on this subject have been published in recent years.[24] Until now, the systems described were always small organic molecules, such as $(TMTSF)_2X$, which form stacks, where TMTSF stands for 2,3,6,7-tetramethyl-1,4,5,8-tetraselenafulvalenium and X for counterions like PF_6^-, ClO_4^-, NO_3^-, etc. On the other hand, our hexamer **1** has a length of about 4.6 nm and,

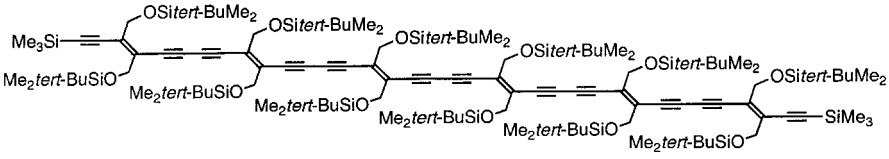

1

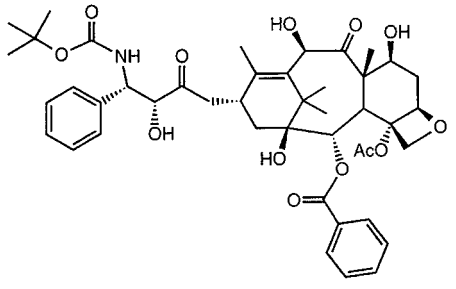

2

SCHEME 1

TABLE I.
ΔH_f for PM3-Optimized Structures of 1 and 2.

Compound	Geometry	Symmetry	π Bonds	ΔH_f (kJ mol^{-1})
1	RHF	C_i	Localized	−118.4
1	RHF	C_2	Localized	−120.9
1	UHF	C_2	''Delocalized''	−121.3
1	UHF	C_i	''Delocalized''	−136.8
2	RHF	C_1	—	−1752.7

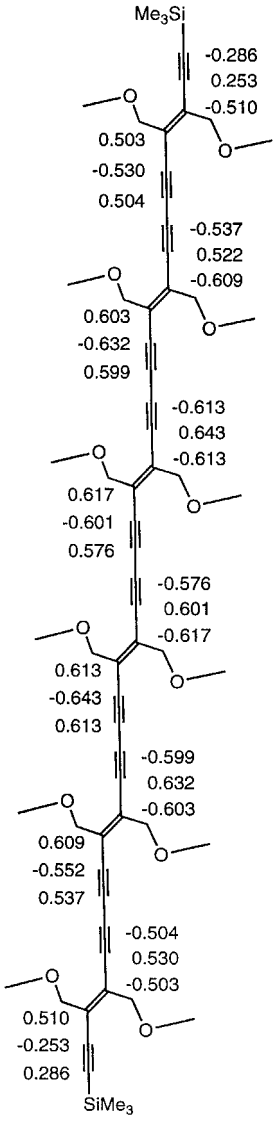

FIGURE 1. The UHF-PM3 spin densities of hexamer **1**. The numbers indicate for this molecule a spin-polarized electronic structure that results from a nonsinglet HF instability. A plus sign indicates an α spin and a minus sign a β spin dominance at the indicated π centers.

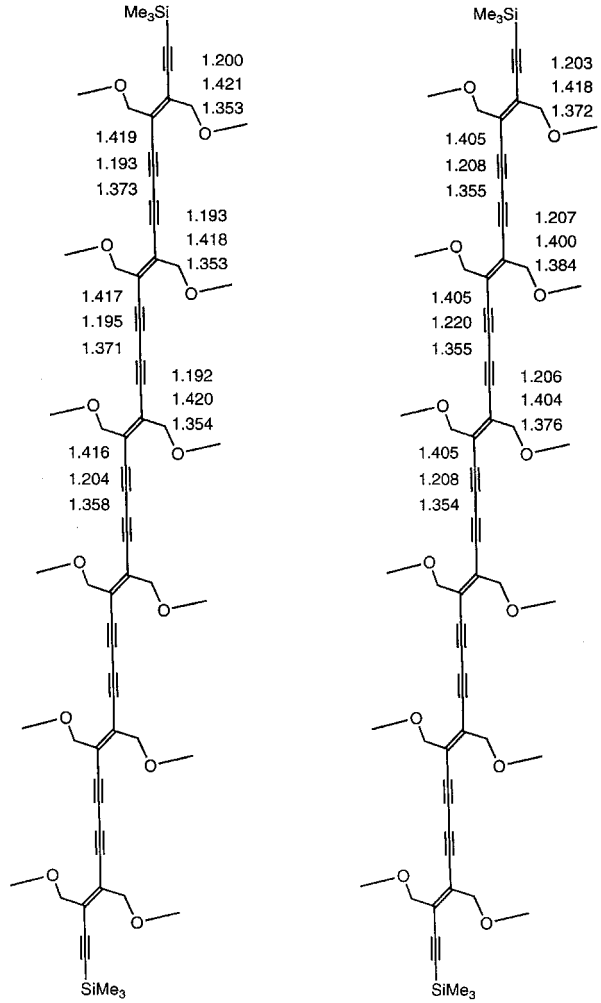

FIGURE 2. The bond lengths equilization in the UHF-PM3-optimized structure of **1** (right side) in comparision with the RHF-PM3-optimized one (left side).

therefore, falls into a category of molecules in which our computations predict SDWs for both conjugated large-ring and long-chain systems. There is hope that the SDW is not an artifact of a semiempirical method, but rather has strong physical background. As mentioned earlier, the semiempirical results for the structure of [18]annulene have recently been confirmed by *ab initio* computations.[16]

In Tables IIa and IIb are given the bond lengths and angles of compound **2** obtained by X-ray crystal analysis[19] and those of the PM3-geometry-optimized structure. Whereas, for bond lengths, satisfactory agreement was observed in a few cases, somewhat larger deviations were obtained for bond angles [the largest being Δ(C2—C1—C14) = 15.8°).

CALCULATED AND EXPERIMENTAL UV/VIS ABSORPTION SPECTRA OF COMPOUNDS 1 AND 2

The lowest energy transition of poly(triacetylene) **1** is covered under a broad, unstructured absorption band. A precise determination of λ_{max} therefore required the deconvolution of the UV/Vis spectrum, yielding a value of 463.6 ± 0.5 nm.[6] In Figure 3 (top) the experimental spectrum of **1** with the three most relevant calculated transitions is given. Table III shows the first 19 computed transitions of **1** as printed out by SIXW.C. The program characterizes these transitions by the occupied and virtual orbitals that define the main electronic configurations of the 19 excited states. As a first step in the theoretical investigation of poly(triacetylene) **1**, we considered

TABLE IIa.
X-Ray and Computed Bond Lengths of Structure 2 (nm) with ESDs in Parentheses.

Bond[a]	X-Ray[a]	PM3	Bond[a]	X-Ray[a]	PM3
C1 — C2	.1573(7)	.1545	O2 — C17′	.1355(8)	.1366
C1 — C14	.1548(7)	.1546	O13 — C1′	.1356(6)	.1363
C1 — C15	.1555(8)	.1596	C1′ — O1′	.1187(8)	.1221
C1 — O1	.1423(6)	.1451	C1′ — C2′	.1493(9)	.1542
C2 — C3	.1560(7)	.1603	C2′ — O2′	.1423(7)	.1408
C2 — O2	.1450(6)	.1431	C2′ — C3′	.1510(9)	.1559
C3 — C4	.1551(7)	.1556	C3′ — C4′	.1517(8)	.1513
C3 — C8	.1558(7)	.1597	C3′ — N10′	.1474(8)	.1487
C4 — C5	.1547(8)	.1576	C4′ — C5′	.1352(8)	.1397
C4 — C20	.1550(7)	.1562	C4′ — C9′	.1394(9)	.1398
C4 — O4	.1428(6)	.1435	C5′ — C6′	.1386(10)	.1392
C5 — C6	.1516(8)	.1512	C6′ — C7′	.1376(11)	.1392
C5 — O5	.1473(7)	.1460	C7′ — C8′	.1356(11)	.1389
C6 — C7	.1514(8)	.1530	C8′ — C9′	.1377(10)	.1391
C7 — C8	.1573(8)	.1592	N10′ — C11′	.1345(9)	.1426
C7 — O7	.1406(7)	.1408	C11′ — O11′	.1214(9)	.1222
C8 — C9	.1570(8)	.1594	C11′ — O12′	.1350(9)	.1355
C8 — C19	.1528(7)	.1522	O12′ — C13′	.1481(9)	.1449
C9 — C10	.1520(7)	.1605	C13′ — C14′	.1487(16)	.1528
C9 — O9	.1201(7)	.1223	C13′ — C15′	.1497(15)	.1529
C10 — C11	.1494(7)	.1507	C13′ — C16′	.1509(19)	.1536
C10 — O10	.1418(7)	.1398	C17′ — O17′	.1228(9)	.1214
C11 — C12	.1351(8)	.1360	C17′ — C18′	.1430(10)	.1487
C11 — C15	.1533(8)	.1508	C18′ — C19′	.1369(14)	.1396
C12 — C13	.1511(8)	.1542	C18′ — C23′	.1428(14)	.1397
C12 — C18	.1506(10)	.1483	C19′ — C20′	.1394(13)	.1390
C13 — C14	.1539(8)	.1582	C20′ — C21′	.1224(27)	.1393
C13 — O13	.1447(7)	.1447	C21′ — C22′	.1391(31)	.1391
C15 — C16	.1523(8)	.1537	C22′ — C23′	.1468(16)	.1391
C15 — C17	.1571(9)	.1554	C24′ — O24′	.1180(7)	.1216
C20 — O5	.1452(7)	.1444	C24′ — C25′	.1462(9)	.1505

[a] Numbering and values taken from ref. 19.

TABLE IIb.
X-Ray and Computed Bond Angles of Structure 2 (°) with ESDs in Parentheses.

Angle[a]	X-Ray[a]	PM3	Angle[a]	X-Ray[a]	PM3
C2 — C1 — C14	109.4(4)	125.2	C11 — C15 — C16	114.6(5)	117.1
C2 — C1 — C15	113.4(4)	113.6	C11 — C15 — C17	109.9(5)	110.8
C2 — C1 — O1	106.2(4)	100.8	C16 — C15 — C17	104.4(5)	99.8
C14 — C1 — C15	111.7(4)	102.7	C4 — C20 — O5	92.4(4)	91.2
C14 — C1 — O1	105.2(4)	100.7	C2 — O2 — C17′	119.6(4)	120.8
C15 — C1 — O1	110.4(4)	113.3	C4 — O4 — C24′	117.2(4)	124.1
C1 — C2 — C3	117.2(4)	114.4	C5 — O5 — C20	90.6(4)	93.6
C1 — C2 — O2	105.2(4)	111.6	C13 — O13 — C1′	115.9(4)	120.3
C3 — C2 — O2	106.6(4)	104.6	O13 — C1′ — O1′	122.7(6)	120.1
C2 — C3 — C4	111.3(4)	105.0	O13 — C1′ — C2′	112.2(5)	111.0
C2 — C3 — C8	116.4(4)	125.7	O1′ — C1′ — C2′	124.9(6)	129.0
C4 — C3 — C8	110.3(4)	112.5	C1′ — C2′ — O2′	107.4(5)	105.8
C3 — C4 — C5	119.8(4)	121.0	C1′ — C2′ — C3′	113.6(5)	111.9
C3 — C4 — C20	119.6(4)	118.1	O2′ — C2′ — C3′	111.0(5)	114.5
C3 — C4 — O4	111.2(4)	105.0	C2′ — C3′ — C4′	108.5(5)	110.2
C5 — C4 — C20	84.4(4)	84.8	C2′ — C3′ — N10′	109.4(5)	111.2
C5 — C4 — O4	111.1(4)	107.9	C4′ — C3′ — N10′	113.3(5)	112.2
C20 — C4 — O4	108.0(4)	119.7	C3′ — C4′ — C5′	122.4(6)	118.8
C4 — C5 — C6	119.2(5)	117.9	C3′ — C4′ — C9′	119.0(5)	121.9
C4 — C5 — O5	91.8(4)	90.3	C5′ — C4′ — C9′	118.4(6)	119.4
C6 — C5 — O5	113.5(5)	112.5	C4′ — C5′ — C6′	120.8(6)	120.3
C5 — C6 — C7	114.0(5)	112.1	C5′ — C6′ — C7′	120.5(7)	120.1
C6 — C7 — C8	111.9(4)	112.4	C6′ — C7′ — C8′	118.9(7)	119.8
C6 — C7 — O7	111.0(5)	105.0	C7′ — C8′ — C9′	120.7(7)	120.2
C8 — C7 — O7	112.4(4)	113.0	C4′ — C9′ — C8′	120.6(7)	120.3
C3 — C8 — C7	104.6(4)	102.5	C3′ — N10′ — C11′	119.2(5)	121.4
C3 — C8 — C9	116.0(4)	116.6	N10′ — C11′ — O11′	126.8(7)	121.2
C3 — C8 — C19	113.6(4)	116.6	N10′ — C11′ — O12′	107.5(6)	113.4
C7 — C8 — C9	103.0(4)	105.4	O11′ — C11′ — O12′	125.5(7)	125.4
C7 — C8 — C19	111.9(4)	107.5	C11′ — O12′ — C13′	120.6(6)	121.3
C9 — C8 — C19	107.3(4)	107.2	O12′ — C13′ — C14′	99.5(7)	102.2
C8 — C9 — C10	123.3(5)	130.6	O12′ — C13′ — C15′	110.7(8)	111.9
C8 — C9 — O9	118.1(5)	116.4	O12′ — C13′ — C16′	109.9(8)	111.9
C10 — C9 — O9	118.0(5)	112.3	C14′ — C13′ — C15′	114.1(9)	111.1
C9 — C10 — C11	112.6(5)	114.8	C14′ — C13′ — C16′	110.4(9)	109.6
C9 — C10 — O10	111.6(5)	107.8	C15′ — C13′ — C16′	111.6(9)	109.7
C11 — C10 — O10	110.3(5)	114.9	O2 — C17′ — O17′	123.5(6)	120.6
C10 — C11 — C12	119.6(5)	128.4	O2 — C17′ — C18′	112.1(6)	111.8
C10 — C11 — C15	120.5(5)	115.7	O17′ — C17′ — C18′	124.4(7)	127.6
C12 — C11 — C15	119.7(5)	114.2	C17′ — C18′ — C19′	121.9(8)	119.2
C11 — C12 — C13	114.9(5)	120.8	C17′ — C18′ — C23′	118.3(8)	120.5
C11 — C12 — C18	127.1(5)	124.8	C19′ — C18′ — C23′	119.7(9)	120.3
C13 — C12 — C18	117.9(5)	114.0	C18′ — C19′ — C20′	118.2(10)	119.6
C12 — C13 — C14	111.3(4)	116.0	C19′ — C20′ — C21′	127.5(16)	120.1
C12 — C13 — O13	109.3(4)	108.7	C20′ — C21′ — C22′	117.5(20)	120.2
C14 — C13 — O13	106.4(4)	107.2	C21′ — C22′ — C23′	121.4(17)	120.2
C1 — C14 — C13	113.9(4)	105.9	C18′ — C23′ — C22′	114.6(11)	119.6
C1 — C15 — C11	105.5(4)	95.5	O4 — C24′ — O24′	123.2(5)	121.6
C1 — C15 — C16	110.0(5)	119.5	O4 — C24′ — C25′	109.7(5)	111.6
C1 — C15 — C17	112.7(5)	114.9	O24′ — C24′ — C25′	127.1(6)	126.7

[a] Numbering and values taken from ref. 19.

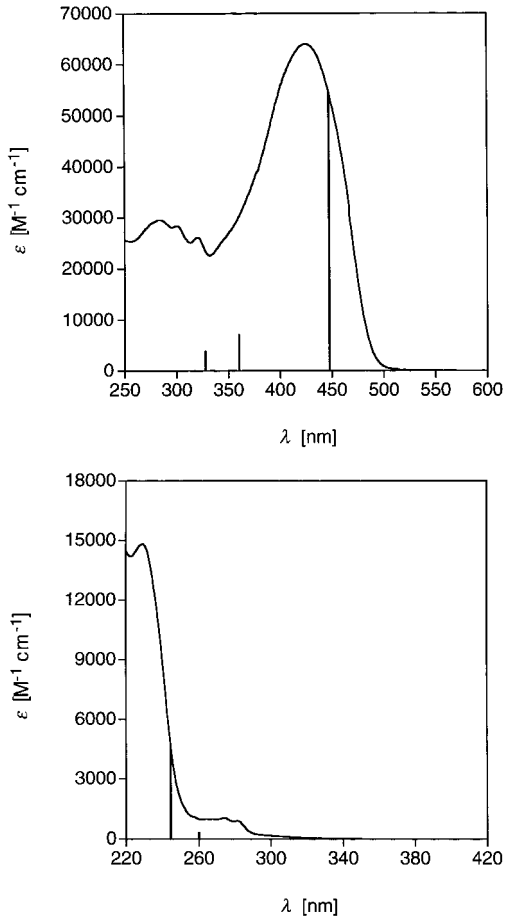

FIGURE 3. The experimental UV / Vis spectra of compounds **1** (top) and **2** (bottom) and the CNDO / S-CI-calculated strongest absorption bands are represented as lines at the appropriate wavelength. In both cases, the most intense transition was normalized to the experimentally measured extinction coefficient.

its first electronic transition. It is characterized by a transition from the occupied orbital 211 of the irreducible representation a_g to the virtual orbital 212 belonging to the irreducible representation a_u. Table IV lists the energies of the theoretical first $a_g \rightarrow a_u$ transitions for the RHF- and UHF-optimized structures, with the corresponding experimental energies of the absorption band of hexamer **1**. It is obvious that the structure computed by UHF shows a first absorption (447 nm) that is closer to the experimental wavelength in the region of 460 nm than the one computed for the RHF structure (398 nm). The main component (60%) of the excited state corresponds, as already stated, to an electronic configuration, which may be interpreted in a pictorial way as the HOMO–LUMO transition represented in Figure 4 (HOMO: bottom, LUMO: top). The theoretically estimated extinction coefficients (RHF-optimized structure: $\varepsilon = 177407$; UHF-optimized structure: $\varepsilon = 181546$) are, although too large, in the approximate order of magnitude of the experimental value of $\varepsilon = 36500$.

Figure 3 (bottom) shows the experimentally determined spectrum with the first two relevant transitions, indicated by lines at the appropriate wavelength. Table V lists the first 19 computed transitions of the natural product **2** as they are provided by output of program SIXW.C. As mentioned earlier, the program characterizes these transitions by the occupied and virtual orbitals, that define the main electronic configurations of the 19 excited states. We have looked more closely at the three first transitions of the antitumoral compound **2**. Because the natural product is of the spatial point group C_1, the transitions cannot be characterized by symmetry. Table VI lists the three first experimental and theoretical transitions of **2**. The main components (54%, 46%, 92%) of the linear combinations of the electronic configurations were represented in a pictorial way as electronic transitions between the occupied and unoccupied orbitals represented in Figure 5. The first is characterized by a transition from occupied orbital 156 to virtual orbital 160. The second is characterized by a transition from occupied orbital 153 to virtual orbital 158. The third transition takes place between occupied orbital 157 to virtual orbital 162. It should be noted that the three transitions occur in three spatially separated locations of the complex molecule, namely the side chain phenyl ring (Fig. 5, left), the main system benzoate substituent (Fig. 5, center), and the main system double bond (Fig. 5, right). The theoretically estimated extinction coefficients ($\varepsilon_1 = 372$; $\varepsilon_2 = 154$; $\varepsilon_3 = 19322$) are, again, of magnitudes comparable to the experimental values of $\varepsilon_1 = 1670$; $\varepsilon_2 = 1730$; $\varepsilon_3 = 14800$.

Conclusions

We have calculated the UV/Vis spectrum of poly(triacetylene) **1**, which is a long, linearly conjugated rod with 36 C-atoms and belongs to a class of compounds that has been getting considerable attention in recent years. These molecules have some common characteristics with the annulenes,

TABLE III.
Calculated Transitions of 1 for UHF Structure with C_i Symmetry.

	Transition		Symmetry		Energy			Intensity	
No.	Occ.[a]	Virt.[b]	Occ.	Virt.	eV	cm^{-1}	nm	f[c]	ε[d] (M^{-1} cm^{-1})
1	211	212	a_g	a_u	2.771	22349	447	3.3632	181546
2	207	212	a_g	a_u	2.880	23228	431	0.0003	15
3	206	212	a_u	a_u	2.965	23913	418	0.0000	0
4	203	212	a_g	a_u	3.073	24790	403	0.0002	9
5	211	213	a_g	a_g	3.086	24896	402	0.0000	0
6	205	213	a_g	a_g	3.322	26798	373	0.0000	0
7	204	213	a_u	a_g	3.326	26830	373	0.0002	9
8	211	214	a_g	a_u	3.441	27756	360	0.4298	23202
9	209	213	a_g	a_g	3.683	29704	337	0.0000	0
10	209	214	a_g	a_u	3.782	30505	328	0.2282	12317
11	211	232	a_g	a_u	3.786	30541	327	0.0166	894
12	211	233	a_g	a_g	3.820	30811	325	0.0000	0
13	211	234	a_g	a_u	3.882	31310	319	0.0006	34
14	210	235	a_u	a_g	4.046	32636	306	0.0010	54
15	210	236	a_u	a_u	4.046	32636	306	0.0000	0
16	210	212	a_u	a_u	4.230	34117	293	0.0000	0
17	210	216	a_u	a_u	4.292	34615	289	0.0000	0
18	210	215	a_u	a_g	4.292	34615	289	0.0014	78
19	211	224	a_g	a_g	4.391	35421	282	0.0000	0

[a] Occ.: occupied orbital.
[b] Virt.: virtual orbital.
[c] Computed according to Ref. 37.
[d] $\varepsilon = f \cdot 2.699 \cdot 10^4 / b$ (b: line width = 0.5).

because, for both classes, it is possible to consider either structures with localized or delocalized π bonds. Whereas for the annulenes, localization or delocalization expresses itself in different symmetry point groups (e.g., [18]annulene delocalized: D_{6h}; localized: D_{3h}) this is not the case for the molecular wires. As the experimental value fits better with the theoretical result for a ''delocalized'' structure, we assume the existence of the spin-density wave predicted by Fukutome. This result is of fundamental interest. Strong support for our result is coming from the fact that, for [18]annulene, the results computed with the same CNDO/S parameter set were recently confirmed by *ab initio* calculations. This indicates that Fukutome's concept of the behavior of long polyenes is probably correct for the poly(triacetylene)s, and seems to be more realistic than the concept of bond-length alternation for long conjugated chains introduced by Longuett-Higgins and Salem. But, as noted earlier, only experiments or high-level *ab initio* calculations will ultimately determine if the

TABLE IV.
Longest Wavelength Absorption of Poly(triacetylene) 1.

	Orbital No.		Absorption Calculated (nm) and Deviation (cm^{-1})		ε Calc. (M^{-1} cm^{-1})		Absorption[b] Experimental (nm)	ε[b] Exp. (M^{-1} cm^{-1})
π Centers	HOMO	LUMO	RHF[a]	UHF[a]	RHF[a]	UHF[a]		
36	211	212	398 $\pm$ 3567	447 $\pm$ 802	177407	181546	463.6 $\pm$ 0.5	36500

[a] RHF: RHF-PM3 geometry optimization; UHF: UHF-PM3 geometry optimization.
[b] Longest wavelength absorption in $CHCl_3$ at room temperature, obtained by deconvolution of the absorption spectrum.[6]

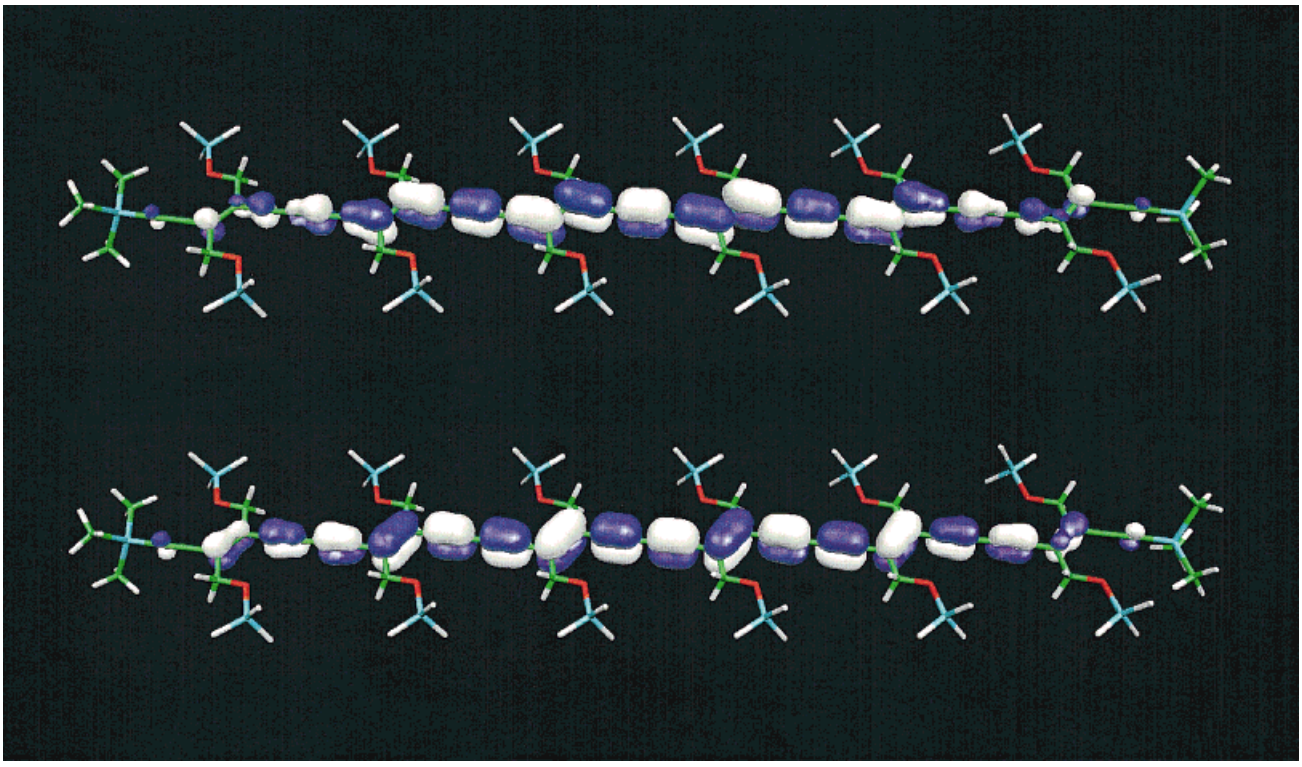

FIGURE 4. The first electronic band of the RHF-PM3- and UHF-PM3- optimized structures of **1** is characterized by a transition from the HOMO (orbital 211, bottom) to the LUMO (orbital 212, top). The orbitals are computed by CNDO / S-CI.

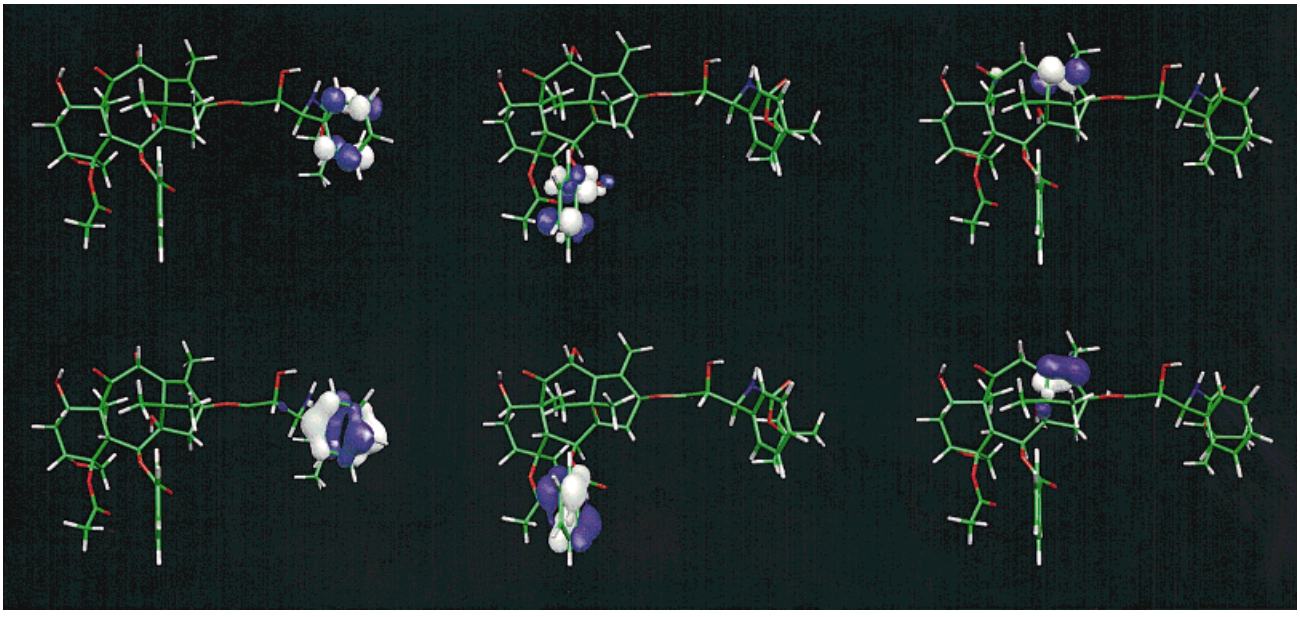

FIGURE 5. The first, second, and third electronic bands of **2** are characterized by transitions from orbital 156 to orbital 160 ($\pi-\pi^*$ transition in the side chain phenyl ring, left), from orbital 153 to orbital 158 ($\pi-\pi^*$ transition in the main system benzoate, center), and from orbital 157 to orbital 162 ($\pi-\pi^*$ transition in the main system double bond, right). HOMO: 157; LUMO: 158. The orbitals are computed by CNDO / S-CI.

TABLE V.
Calculated Transitions of 2 C_1 Symmetry.

No.	Transition		Energy			Intensity	
	Occ.[a]	Virt.[b]	(eV)	(cm^{-1})	(nm)	f[c]	ε[d] (M^{-1} cm^{-1})
1	156	160	4.772	38489	260	0.0069	372
2	153	158	4.798	38704	258	0.0029	154
3	157	162	5.069	40890	245	0.3580	19323
4	157	158	5.302	42766	234	0.0010	55
5	157	167	5.732	46232	216	0.0072	389
6	157	159	5.823	46968	213	0.0004	19
7	154	158	5.866	47317	211	0.1281	6914
8	157	164	5.895	47549	210	0.0034	183
9	156	161	5.934	47867	209	0.0711	3836
10	157	160	6.174	49799	201	0.0004	21
11	152	167	6.205	50048	200	0.0070	375
12	157	161	6.232	50265	199	0.0016	88
13	151	162	6.545	52790	189	0.0744	4016
14	153	159	6.681	53888	186	0.6479	34971
15	154	159	6.739	54357	184	0.5059	27307
16	155	160	6.773	54635	183	1.2537	67674
17	157	163	6.790	54768	183	0.0246	1327
18	155	161	6.803	54872	182	1.4287	77121
19	144	158	6.891	55581	180	0.0078	422

[a] Occ.: occupied orbital.
[b] Virt.: virtual orbital.
[c] Computed according to Ref. 37
[d] $\varepsilon = f \cdot 2.699 \cdot 10^4 / b$ (b: line width = 0.5).

typical undulating spin-density distribution has physical meaning or is an artifact of the one determinant approach.

In addition, the three first electronic transitions of molecule **2**, a large nonplanar three-dimensional structure, have been computed. It is of interest that the three transitions are localized in three different, spatially separated chromophores of the large molecule. As the correspondence between the experimental and computed transition energy is rather good, we can assume that our computation is correct. This will lead to a better understanding of the photochemical behavior of this large natural product.

Finally, we believe that the program presented in this work is a useful tool for the theoretical interpretation of the UV/Vis spectra for a wide variety of large organic molecules.

Acknowledgments

We are very grateful to Prof. Dr. Françoise Gueritte-Voegelein for providing an authentic sample of **2** for recording the UV/Vis spectrum. We also thank Prof. Dr. Peter Chen for his generous support of this work. The computations were performed on the workstation cluster in his labora-

TABLE VI.
First Three Absorptions of 2.

Location	Main Transition		Absorption Calc. (nm)	ε Calc. (M^{-1} cm^{-1})	Absorption[c] Exp. (nm)	ε[c] Exp. (M^{-1} cm^{-1})
	Occ.[a]	Virt.[b]				
Side chain phenyl	156	160	260	372	283	1670
Ring system benzoate	153	158	258	154	275	1730
Ring system double bond	157	162	245	19323	230	14800

[a] Occ.: occupied orbital (HOMO: 157).
[b] Virt.: virtual orbital (LUMO: 158).
[c] Taken from ref. 18.

tory (including IBM, DEC, and Silicon Graphics computers), which was installed by Supercomputing Systems AG. Contributions to the C programs by Dr. Josef Heinzer and Mr. Derek Feichtinger and the literature search of Mr. Josef Meienberger are gratefully acknowledged. The orbitals were represented with program MOLEKEL by Dr. Peter Flükiger, who kindly programmed an interface to the numerical output of SIXW.C. Finally, we thank Prof. Akira Igawa and Prof. Atsumu Ohmura for providing a complete publication list of Prof. Hideo Fukutome.

Appendix

DESCRIPTION OF THE PROGRAM

The program consists of several groups of procedures to monitor: (1) the graphical X WINDOWS user interface; (2) the allocation and freeing of the memory space; (3) the POSTSCRIPT output of the UV/Vis spectrum; and (4) the computational processes as well as defining the one-center integrals (see Table VII).[25–27] An input example is available as Supplementary Material.

For the two center integrals is used the Nishimoto–Mataga [28] or the Ohno–Klopman[29] approximation, eq. (1a,b) (interatomic distance R [Å], electron repulsion integral γ_{XY} [eV]):

$$\gamma_{AB} = 14.3942/((R_{AB} + (14.3942/2\gamma_{AA}) + (14.3942/2\gamma_{BB})) \quad (1a)$$

$$\gamma_{AB} = 14.3942/\left((R_{AB}^2 + ((14.3942/2\gamma_{AA}) + (14.3942/2\gamma_{BB}))^2\right)^{1/2} \quad (1b)$$

$$\gamma_{AA} = (\varphi_\mu \varphi_\mu \mid \varphi_\nu \varphi_\nu) \quad \mu, \nu \in A$$

$$\gamma_{AB} = (\varphi_\mu \varphi_\mu \mid \varphi_\nu \varphi_\nu) \quad \mu \in A;\ \nu \in B$$

Computation of the resonance integrals is accomplished by the Mulliken approximation[30]:

$$Hij = 0.5(\beta_A^0 + \beta_B^0)S_{ij}; \quad i \in A,\ j \in B \quad (2)$$

For the (p–p) π integrals β_π^0 and for the (p–p) σ integrals β_σ^0 is used. β_π^0 is chosen proportional to

TABLE VII.
Parameterization of One-Center Integrals.

Atom	$-0.5\,(I_\mu + A_\mu)$ (eV) s	p	$-\beta_A^0$ (eV)	Slater Exponent	$\gamma_{AA}z_A$ (eV)(a.u.)
H	7.175	—	12.0	1.2	12.851
Li	3.105	2.05	3.0	.65	2.981
Be	6.55	3.035	4.0	.975	5.852
B	10.305	4.37	5.0	1.3	8.103
C	14.960	5.805	17.5	1.625	10.934
N	20.485	8.480	26.0	1.950	13.105
O	27.255	10.965	45.0	2.275	15.276
F	28.480	12.180	50.0	2.600	17.367
Na	2.805	1.565	5.0	.733	2.951
Mg	5.875	2.29	1.0	.95	4.462
Al	8.595	3.92	1.5	1.167	5.13
Si	12.125	6.005	5.25	1.383	6.374
P	14.34	7.235	7.8	1.6	9.315
S	15.81	8.41	13.5	1.817	10.016
Cl	17.5	9.38	15.0	2.033	11.37
Ge	11.435	4.080	7.5	1.4125	5.174
As	13.335	5.345	9.75	1.575	8.035
Se	16.315	7.1	12.0	1.7375	9.166
Br	19.63	8.4	16.5	1.9	9.47
In	9.215	3.335	10.3	1.25	5.673
Sn	12.14	3.905	11.9	1.4125	2.994
Sb	13.155	4.965	12.5	1.575	8.065
Te	14.935	6.81	13.8	1.738	11.876
I	15.69	8.095	15.2	1.9	9.157

β_σ^0 (del Bene–Jaffé)[1c]:

$$\beta_\pi^0 = 0.585\ \beta_\sigma^0 \tag{3}$$

As a first step, a SCF–LCAO–MO computation is performed for the determination of the eigenvectors **u** and the eigenvalues **e**. We are starting with the secular determinant:

$$|\mathbf{Fu} - \mathbf{ue}| = 0 \tag{4}$$

The Fock matrix is computed iteratively starting with the approximation **F°**. The procedure is interrupted, as soon as the electronic energy varies within a fixed threshold.

The elements of the Fock matrix can be written with the CNDO approximation by Pople and Segal, and can be given by[31]:

$$\begin{aligned} F_{\mu\mu} &= H_{\mu\mu}^{\text{core}} - 0.5P_{\mu\mu}\gamma_{AA} + \sum_B P_{BB}\gamma_{AB} \\ H_{\mu\mu} &= -0.5(I_\mu + A_\mu) - (z_A - 0.5)\gamma_{AA} \\ &\quad - \sum_{B\neq A} z_B\gamma_{AB} \\ F_{\mu\nu} &= H_{\mu\nu}^{\text{core}} - 0.5P_{\mu\nu}\gamma_{AB} \\ H_{\mu\nu}^{\text{core}} &= \beta_{AB}^0 S_{\mu\nu} \\ I_\mu &= \text{valence ionization potential} \\ A_\mu &= \text{electron affinity} \\ z_A &= \text{charge at the nucleus } A \end{aligned} \tag{5}$$

The electronic energy is given by:

$$E_{\text{tot}}^{\text{el}} = 0.5\sum_{\mu,\nu}^{n} P_{\mu\nu}(F_{\mu\nu} + H_{\mu\nu}^{\text{core}}) \tag{6}$$

$$\begin{aligned} P_{\mu\nu} &= \sum_i^{\text{occ}} u_{i\mu}u_{i\nu}b_i \\ b_i &= \text{occupation number of the } i\text{th MO} \\ u_{i\mu} &= \mu\text{th element of the } i\text{th eigenvector} \end{aligned} \tag{7}$$

For the improvement of the convergence in critical cases, it is possible to apply the Hartree extrapolation.[32] Computation of the eigenvalues and eigenvectors of a real symmetric matrix is accomplished by transformation to tridiagonal form (Householder tridiagonal reduction),[33a] diagonalization of the tridiagonal matrix with the QL method, and backtransformation of the eigenvectors to those of the original matrix (tridiagonal QL implicit).[33b]

To be able to accomplish the Mulliken population analysis, the eigenvectors of the special eigenvalue problem (4) have to be transformed to those of the general one[34]:

$$\mathbf{F}^a\mathbf{v} - \mathbf{Sve} = 0 \tag{8}$$

For this purpose, we use the relations:

$$\mathbf{v} = \mathbf{cD}^{-1/2}\mathbf{c}^T\mathbf{u};\ \mathbf{Sc} = \mathbf{cD} \tag{9}$$

where **S** is the overlap matrix, **c** is the eigenvector of the overlap matrix, and **D** is the eigenvalue of the overlap matrix.

The total and the reduced overlap population matrix [eq. (10a,b)], the charge matrix [eq. (11)], the net [eq.(12a)], and gross atom charges [eq. (12b)] can now be calculated:

$$p_{\mu\nu} = \sum_i^{\text{occ}} b_i v_{i\mu}v_{i\nu}S_{\mu\nu};\ p_{AB} = \sum_{\substack{\mu\in A\\ \nu\in B}} p_{\mu\nu} \tag{10a,b}$$

$$p_{i\mu} = v_{i\mu}\sum_\nu S_{\mu\nu}v_{i\nu} \tag{11}$$

$$q_\mu = \sum_i^{\text{occ}} p_{i\mu};\ q_A = \sum_{\mu\in A} q_\mu \tag{12a,b}$$

for the calculation of the electron transitions we have to establish a configuration interaction matrix and to diagonalize it. The following configurations are considered: a ground configuration [eq. (13)], and singly excited configurations [eqs. (14) and (15)].

Type 0: Ground configuration:

$$^1X_0 = |1\bar{1}\cdots n\bar{n}| \tag{13}$$

Type 1: Singly excited configurations:

$$^1X_r^s = 1/\sqrt{2}\,(|r\bar{s}| + |s\bar{r}|) \tag{14}$$

$$^3X_r^s = 1/\sqrt{2}\,(|r\bar{s}| - |s\bar{r}|) \tag{15}$$

Energy of the singly excited configurations:

$$E\left(^1X_r^s\right) - E\left(^1X_0\right) = \varepsilon_s - \varepsilon_r - (rr\mid ss) + 2(rs\mid rs) \tag{16}$$

$$E\left(^3X_r^s\right) - E\left(^1X_0\right) = \varepsilon_s - \varepsilon_r - (rr\mid ss) \tag{17}$$

Interaction energies of the configurations among each other:

$$\left\langle ^1X_r^s|\hat{H}|^1X_t^u\right\rangle = \delta_{su}\cdot F_{rt} - \delta_{rt}\cdot F_{su} - (rs\mid tu) + 2(rt\mid su) \tag{18}$$

$$\left\langle ^1X_r^s|\hat{H}|^1X_0\right\rangle = F_{rs} \tag{19}$$

$$\left\langle ^3X_r^s|\hat{H}|^3X_t^u\right\rangle = \delta_{su}\cdot F_{rt} - \delta_{rt}\cdot F_{su} - (rs\mid tu) \tag{20}$$

The energies and interactions of these configurations are calculated and the states of the molecules are represented as linear combinations of these configurations:

$$\Psi_i = \sum_j c_{ij} X_j \tag{21}$$

The computation of the different types of the doubly excited singlet configurations [35] represents, together with the calculation of their interactions, the proper extension of the method:

Type 1:

$$^1X_{hh}^{ll} = |l\bar{l}| \tag{22}$$

Type 2:

$$^1X_{hh}^{lm} = 1/\sqrt{2}\,(|l\bar{m}| - |\bar{l}m|) \tag{23}$$

Type 3:

$$^1X_{hk}^{mm} = 1/\sqrt{2}\left(|h\bar{k}m\bar{m}| - |\bar{h}km\bar{m}|\right) \tag{24}$$

Type 4:

$$^1X_{hk}^{lm} = 1/2\Big(|\bar{h}k\bar{l}m| - |\bar{h}kl\bar{m}| - |h\bar{k}\bar{l}m| + |h\bar{k}l\bar{m}|\Big) \tag{25}$$

Type 5:

$$^1X_{hk}^{lm} = 1/\sqrt{12}\left(2|\bar{h}\bar{k}lm| - |\bar{h}k\bar{l}m| - |\bar{h}kl\bar{m}| - |h\bar{k}\bar{l}m| - |h\bar{k}l\bar{m}| - 2|hk\bar{l}\bar{m}|\right) \tag{26}$$

The energies of the doubly excited configurations can be written in the following way:

$$E\left(^1X_{hh}^{ll}\right) - E\left(^1X_0\right) = 2E\left(^1X_h^l\right) - 2J_{hl} - 2K_{hl} + J_{ll} + J_{hh} \tag{27}$$

$$E\left(^1X_{hh}^{lm}\right) - E\left(^1X_0\right) = E\left(^1X_h^l\right) + E\left(^1X_h^m\right) - J_{hm} + J_{hh} + J_{lm} - J_{lh} - K_{hm} - K_{lh} + K_{lm} \tag{28}$$

$$E\left(^1X_{hk}^{mm}\right) - E\left(^1X_0\right) = E\left(^1X_h^m\right) + E\left(^1X_k^m\right) + J_{mm} - K_{mk} - K_{mh} + J_{hk} - K_{hk} - J_{mh} - J_{mk} \tag{29}$$

$$E\left(^1X_{hk}^{lm}\right) - E\left(^1X_0\right) = E\left(^1X_h^l\right) + E\left(^1X_k^m\right) - 1.5(K_{lh} + K_{mk}) + J_{hk} + J_{lm} - J_{mh} - J_{lk} + 0.5(K_{mh} + K_{lk}) + (K_{lm} + K_{hk}) \tag{30}$$

$$E\left(^1X_{hk}^{lm}\right) - E\left(^1X_0\right) = E\left(^1X_h^l\right) + E\left(^1X_k^m\right) - 0.5(K_{lh} + K_{mk}) + J_{hk} + J_{lm} - J_{mh} - J_{lk} + 1.5(K_{mh} + K_{lk}) - (K_{lm} + K_{hk}) \tag{31}$$

The transition moments from the ground state to these states is given as follows:

$$\langle \Psi_0|\hat{M}|\Psi_i\rangle = \sum_j c_{0j} \sum_k c_{ik} \langle X_j|\hat{M}|X_k\rangle \tag{32}$$

Of the integral on the right side there are three types, namely:

Type 1: $X_j = X_k$: Dipole moment of configuration j:

$$\vec{D}_{jj} = \sum_i^n \langle \psi_i|\hat{M}|\psi_i\rangle b_i(j) - \sum_A z_A \vec{r}_A \tag{33}$$

Type 2: X_j differs from X_k by one MO: transition moment of configuration j to k:

$$\vec{D}_{jk} = \langle \psi_l|\vec{M}|\psi_m\rangle \tag{34}$$

Type 3: X_j differs from X_k by more than one MO:

$$\vec{D}_{jk} = 0 \tag{35}$$

As simplification in this version of the program the ground state was assumed to be identical to the ground configuration in eq. (13), which leads to the transition moment:

$$\langle \Psi_0|\hat{M}|\Psi_i\rangle \approx \sum_k c_{ik} \langle X_0|\hat{M}|X_k(i)\rangle = \sum_k c_{ik} \langle \psi_k(0)|\hat{M}|\psi_k(i)\rangle \tag{36}$$

where $\Psi_k(0)$ is the occupied orbital in the ground configuration and $\Psi_k(i)$ is the occupied orbital of the excited configuration. The oscillator strength is given by [36]:

$$f_{0i} = 8.745 \cdot 10^{-2}\, \bar{\nu}_{0i} |M_{0i}|^2 \tag{37}$$

where $\bar{\nu}_{0i}$ is the mean wave number of the absorption band (eV) and M_{0i} is the transition moment, charge (a.u.), coordinates (Å).

In the LCAO formulation, the integral on the right-hand side of eq. (36) can be rewritten as follows:

$$\langle \psi_0 | \hat{M} | \psi_k \rangle = \sum_{\mu} \sum_{\nu} c_{0\mu} c_{k\nu} \langle \varphi_\mu | \hat{M} | \psi_\nu \rangle; \quad \hat{M} = (x, y, z) \quad (38)$$

The electronic transition moments are computed according to Ellis et al.[37] to obtain nonzero $\sigma-\pi^*$ and $n-\pi^*$ transitions.

References

1. (a) del Bene, J.; Jaffé, H. H. J Chem Phys 1968, 48, 1807–1813; (b) Baumann, H. QCPE Program 333, 1977; (c) PC versions: Buemi, G. CN90AT, CN135AT, QCMP Program 062, 1989; Mishra, P. C. CNDUPC, QCMP Program 064, 1989; Kihara, H. Japan Chemistry Program Exchange # P084, 1993.
2. (a) Kuzmani, H.; Mehring, M.; Roth, S., eds. Electronic Properties of Conjugated Polymers III: Basic Models and Applications; Springer: Berlin, 1989; (b) Miller, J. S. Adv Mater 1993, 5, 671–676; (c) Skotheim, T. A., ed. Handbook of Conducting Polymers. Vols 1, 2; Marcel Dekker: New York, 1986; (d) Salaneck, W. R.; Lundström, I.; Rånby, B., eds. Conjugated Polymers and Related Materials. The Interconnection of Chemical and Electronic Structure; Oxford University Press: Oxford, 1993; (e) Liphardt, M.; Goonesekera, A.; Jones, B. E.; Ducharme, S.; Takacs, J. M.; Zhang, L. Science (Wash, DC), 1994, 263, 367–369, (f) Greenham, N. C.; Moratti, S. C.; Bradley, D. D. C.; Friend, R. H.; Holmes, A. B. Nature 1993, 365, 628–630; (g) Buckley, A. Adv Mater 1992, 4, 153–158; (h) Nalwa, H. S. Adv Mater 1993, 5, 341–358; (i) Berggren, M.; Inganäs, O.; Gustafsson, G.; Rassmusson, J.; Andersson, M. R.; Hjertberg, T.; Wennerström, O. Nature (Lond) 1994, 372, 444–446; (j) Brédas, J.-L. Adv Mater 1995, 7, 263–274.
3. (a) Jones, L., II; Pearson, D. L.; Schumm, J. S.; Tour, J. M. Pure Appl Chem 1996, 68, 145–148; (b) Tour, J. M. Chem Rev 1996, 96, 537–553; (c) Ward, M. D. Chem Ind (Lond) 1996, 15, 568–573.
4. (a) Meier, H.; Stalmach, U.; Kolshorn, H. Acta Polym 1997, 48, 379–384; (b) Müllen, K. Pure Appl Chem 1993, 65, 89–96; (c) Tour, J. M.; Wu, R. Macromolecules 1992, 25, 1901–1907; (d) Roncali, J. Chem Rev 1992, 92, 711–738.
5. (a) Jenekhe, S. A. Macromolecules 1990, 23, 2848–2854; (b) Grimme, J.; Kreyenschmidt, M.; Uckert, F.; Müllen, K.; Scherf, U. Adv Mater 1995, 7, 292–295; (c) Brédas, J. L.; Silbey, R.; Boudreaux, D. S.; Chance, R. R. J Am Chem Soc 1983, 105, 6555–6559; (d) Guay, J.; Kasai, P.; Diaz, A.; Wu, R.; Tour, J. M.; Dao, L. H. Chem Mater 1992, 4, 1097–1105.
6. Martin, R. E.; Gubler, U.; Boudon, C.; Gramlich, V.; Bosshard, C.; Gisselbrecht, J.-P.; Günter, P.; Gross, M.; Diederich, F. Chem Eur J 1997, 3, 1505–1512.
7. Schreiber, M.; Anthony, J.; Diederich, F.; Spahr, M. E.; Nesper, R.; Hubrich, M.; Bommeli, F.; Degiorgi, L.; Wachter, P.; Kaatz, P.; Bosshard, C.; Günter, P.; Colussi, M.; Suter, U. W.; Boudon, C.; Gisselbrecht, J.-P.; Gross, M. Adv Mater 1994, 6, 786–790.
8. (a) Eastmond, R.; Johnson, T. R.; Walton, D. R. M. Tetrahedron 1972, 28, 4601–4616; Diederich, F.; Rubin, Y. Angew Chem 1992, 104, 1123–1146 and Angew Chem Int Ed Engl 1992, 31, 1101–1123.
9. Longuet-Higgins, H. C.; Salem, L. Proc R Soc 1959, A251, 172–185.
10. For a systematic discussion of the Hartree–Fock instabilities see, e.g.: Fukutome, H. Int J Quantum Chem 1981, 20, 955–1065, and references therein. The terms ''singlet'' and ''triplet'' instability were introduced by: Cizek J.; Paldus, J. J Chem Phys 1967, 47, 3976–3985. ''Triplet'' was later replaced by the same authors by the better term ''nonsinglet'' instability: Paldus, J.; Cizek, J. J Chem Phys 1970, 52, 2919–2936.
11. Fukutome, H. Progr Theor Phys 1968, 40, 998–1012, 1227–1245.
12. Matsubara, T.; Yokota, T. In: Proceedings of the International Conference on Theoretical Physics, Kyoto–Tokyo, Japan, 1953, p 693.
13. Bogoliubov, N. N.; Tolmachev, V. V.; Shirkov, D. V. A New Method in the Theory of Superconductivity; Consultant's Bureau: New York, 1959.
14. Baumann, H. J Am Chem Soc 1978, 100, 7196–7201.
15. Dewar, M. J. S.; Haddon, R. C.; Student, P. J. J Chem Soc Chem Commun 1974, 569–570.
16. Choi, C. H.; Kertesz, M.; Karpfen, A. J Am Chem Soc 1997, 119, 11994–11995.
17. Wani, M. C.; Taylor, H. L.; Wall, M. E.; Coggon, P.; McPhail, A. T. J Am Chem Soc 1971, 93, 2325–2327. For reviews, see, e.g.: Guénard, D.; Guéritte-Voegelein, F.; Potier, P. Acc Chem Res 1993, 26, 160–167; Nicolaou, K. C.; Dai, W.-M.; Guy, R. K. Angew Chem 1994, 106, 38–69 and Angew Chem Int Ed Engl 1994, 33, 15–44; Nicolaou, K. C.; Guy, R. K.; Potier, P. Spektrum der Wissenschaft 1996, 8, 76–80.
18. Mangatal, L.; Adeline, M.-T.; Guénard, D.; Guéritte-Voegelein, F.; Potier, P. Tetrahedron 1989, 45, 4177–4190.
19. Guéritte-Voegelein, F.; Guénard, D.; Mangatal, L.; Potier, P.; Guilhem, J.; Cesario, M.; Pascard, C. Acta Crytallogr C Cryst Struct Commun 1990, C46, 781–784.
20. Baker, J. K. Spectrosc Lett 1992, 25, 31–48.
21. Williams, H. J.; Scott, A. I.; Dieden, R. A.; Swindell, C. S.; Chirlian, L. E.; Francl, M. M.; Heerding, J. M.; Krauss, N. E. Can J Chem 1994, 72, 252–260.
22. Pauncz, P. J Mol Struct (Theochem) 1989, 199, 257–263.
23. Bechgaard, K.; Jacobsen, C. S.; Mortensen, K.; Pedersen, H. J.; Thorup, N. Solid State Commun 1980, 33, 1119–1125.
24. (a) Sambongi, T.; Nomura, K. In: Aoki, H.; Tsukada, M.; Schlüter, M.; Lévy, F., eds. New Horizons in Low-Dimensional Electron Systems; Kluwer: Dordrecht, 1992, p 401; (b) Cowan, D. O.; Fortkort, J. A.; Metzger, R. M. In: Metzger, R. M.; Day, P.; Papavassiliou, G. C., eds. Lower-Dimensional Systems and Molecular Electronics; Plenum: New York, 1989, p 1; (c) p 245; (d) p 251.
25. Hinze, J.; Jaffé, H. H. J Phys Chem 1963, 67, 1501–1506.

26. Kuehnlenz, G. W. PhD Thesis, University of Cincinnati, Cincinnati, OH, 1963.
27. Hase, H. L.; Schweig, A. Theor Chim Acta 1973, 31, 215–220.
28. Nishimoto, K.; Mataga, N. Z Phys Chem (NF) 1957, 12, 335–338.
29. Ohno, K. Theor Chim Acta 1964, 2, 219–227; Klopman, G. J Am Chem Soc 1965, 87, 3300–3303.
30. Mulliken, R. S. J Chim Phys 1949, 46, 497–542, 675–713.
31. Pople, J. A.; Segal, G. A. J Chem Phys 1966, 44, 3289–3296.
32. Hartree, D. R. The Calculation of Atomic Structures; Wiley: New York, 1957, p 87. See also: Roothaan, C. C. J.; Bagus, P. S. In: Alder, B.; Fernbach, S.; Rotenberg, M., eds. Methods in Computational Physics, Advances in Research and Applications. Vol 2; Academic: New York, 1963, p 47.
33. (a) Press, W. H.; Flannery, B. P.; Teukolsky, S. A.; Vetterling, W. T. Numerical Recipes in C: The Art of Scientific Computing; Cambridge University Press: Cambridge, UK; 1992, p 469, (b) p 475.
34. Mulliken, R. S. J Chem Phys 1955, 23, 1833–1840, 1841–1846.
35. Straub, P. A. Private communication.
36. See, e.g.: Murrell, J. N. Elektronenspektren organischer Moleküle, BI Hochschultaschenbücher; Mannheim: Zürich, 1967.
37. Ellis, R. L.; Kuehnlenz, G.; Jaffé, H. H. Theor Chim Acta 1972, 26, 131–140.